Max-Planck-Institut
für Meteorologie

REPORT No. 164

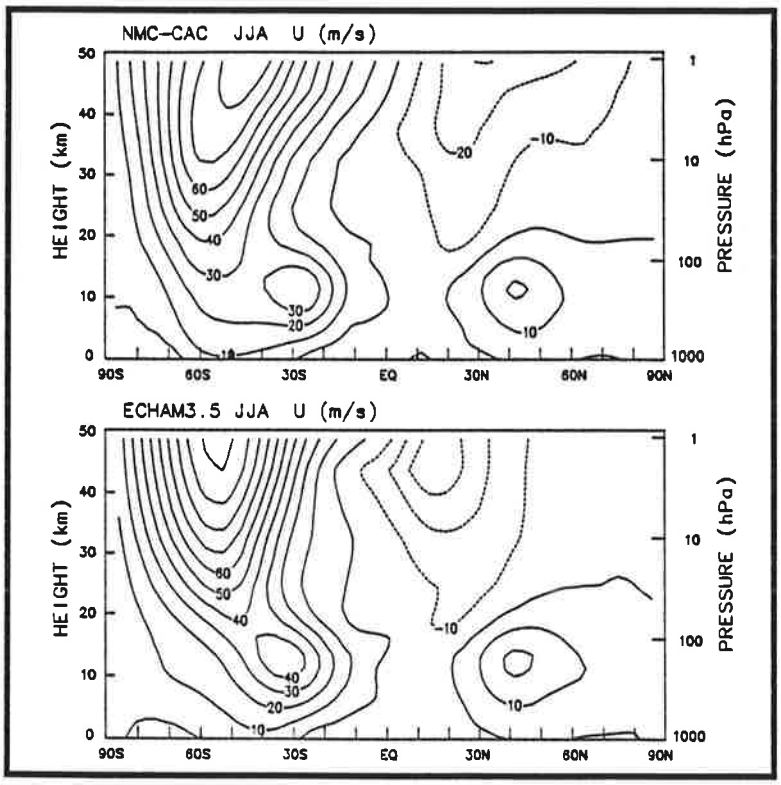

STRATOSPHERIC CLIMATE AND VARIABILITY FROM A GENERAL CIRCULATION MODEL AND OBSERVATIONS. PART II: RESULTS FOR MARCH-MAY, JUNE-AUGUST AND SEPTEMBER-NOVEMBER.

by

ELISA MANZINI • LENNART BENGTSSON

HAMBURG, May 1995

ISSN 0937 – 1060

ISSN 0937 – 1060

Stratospheric climate and variability from a general circulation model and observations. Part II: Results for March-May, June-August and September-November.

Elisa Manzini and Lennart Bengtsson
Max Planck Institute for Meteorology
Hamburg, Germany

Abstract

This report is the second part of a work aimed at studying the climate and variability of the large scale stratospheric circulation by comparing atmospheric statistics from a simulation performed with a general circulation model and from global analyzed observations. Part I (Manzini and Bengtsson, 1994) focused on December-February, while here the remaining part of the seasonal cycle is discussed.

The March-May climatological seasonal mean zonal mean circulation is found to be reasonably well simulated. In the Northern hemisphere stratosphere, very weak westerly winds and high interannual variability characterize both the observed and model data, suggesting that the final stratospheric warming in the Northern hemisphere occurs in a realistic way in the model.

The simulation of the zonal mean circulation during the June-August is relatively successful, although a winter cold bias of moderate amplitude and vertical extent is found. In comparison with the boreal winter, the interannual variability of the austral winter is smaller at high latitudes, in the simulation as well as in the observed state. Although the structure of the observed variability is captured by the model, its magnitude is underestimated, especially in August.

Significant discrepancies between the model results and the analyzed observations are found during the final vortex breakdown (September-November) in the Southern hemisphere, apparently caused by insufficient large scale orographic forcing from the Antarctic continent in the current low resolution model.

1. Introduction

Most of the previous works concerning the evaluation of the stratospheric climate simulated by a general circulation model focused on the December-February and, in fewer cases, June-August periods (for instance, Boville, 1991; Rind et al. 1988a,b; Deque et al. 1994; Hamilton, 1995; and Hamilton et al. 1995). It is interesting to extend the evaluation of the performance of a simulation to the full annual cycle, in order to assess the ability of general circulation models to represent the forming and breakdown of the polar night vortex. In particular, the study of the breakdown of the polar vortex is motivated by the recognized importance of the complex interactions between dynamics, radiation and chemistry, that can lead for instance to the formation of the ozone hole in the Southern Hemisphere (Farman et al. 1985).

It is the purpose of the current work to report of a full annual cycle, long term integration performed with a general circulation model. The simulation results are discussed in two papers: Part I (Manzini and Bengtsson (1994), hereafter MB94), where the general circulation model used (i.e., the so called ECHAM3.5 model) is described and results for December, January and February (DJF) are presented; and current Part II, covering the model performance for the remaining seasons. The performance of the model is studied by comparing basic statistics computed from the simulations with that derived from global analyzed observations.

MB94 found that the December-February climatological seasonal mean, zonal mean circulation was reasonably well captured by the ECHAM3.5 model. In particular, the simulated zonal mean circulation was characterized by weak zonal winds in the lower stratosphere, so that the tropospheric subtropical jet was clearly separated from the stratospheric westerly wind jet in the Northern hemisphere. However, in early winter the polar stratospheric westerly jet was somewhat too confined to high latitudes and a moderate cold bias in the polar lower stratosphere and upper troposphere (5-10°K) was found in the model. The quasi-stationary planetary waves known to dominate the Northern hemisphere stratospheric circulation in winter were generally well captured by the long term time averaged fields of the model. While the simulated monthly interannual variability agreed with that computed from global analyzed observations during January and February, it was underestimated during December, particularly in the upper troposphere and, locally, in the lower stratosphere.

Following MB94, the evaluation of the ECHAM3.5 simulation concentrates on the large scale long term time average and the low frequency interannual variability. Note that as in MB94, long term time averages are presented for seasonal means, while the low frequency interannual variability is computed and presented on a monthly basis. Given that the analyses of daily variability is not included in the current work, the monthly interannual variability will hereafter be simply referred to as interannual variability.

The ECHAM3.5 model was specifically developed for the simulation of the climate of the stratosphere. It is a vertical extension (new top: 0.1 hPa) and a modified version of the ECHAM3 general circulation model (Roeckner et al. 1992). It is also part of a more general project aimed at developing the ECHAM4 general circulation model. Among the several major modifications included in the ECHAM4 model, the new radiation scheme (Morcrette, 1991) and the semi-Lagrangian transport of water vapor and liquid water (Rasch and Williamson, 1990) were implemented into the ECHAM3.5 model. For a detailed description of the ECHAM3.5 model see MB94.

The specifics of the climate simulation performed are to be found in MB94, and are here only briefly summarized:
(i) The simulation consisted of a 20-year integration including the annual cycle in solar radiation and in climatological sea surface temperatures;
(ii) Diurnal cycle in solar radiation and gravity wave drag were excluded;
(iii) A three-layer Rayleigh friction was applied at the top of the model, above 1hPa;
(iv) A $2d\nabla^4$ horizontal diffusion operator was used throughout all the atmosphere.

The dataset of global analyzed observations consists of monthly mean geopotential height and derived temperature and zonal wind fields at 17 vertical levels from 1000 to 1 hPa. The dataset was kindly provided by W. Randel. For description of the dataset see Randel (1992) and also MB94, and references therein.

The paper is organized as follow. Section 2 presents results for March, April and May (MAM), with a discussion of the final breakdown of the Northern hemisphere polar vortex. Section 3 deals with June, July and August (JJA), focusing on the evaluation of the Southern hemisphere winter simulation. September, October and November (SON) and the breakdown of the Southern hemisphere polar vortex are presented in Section 4. Conclusions are found in Section 5.

2. The March - May period

The MAM zonal mean temperature for the 12 year NMC-CAC analyses and for the 20 year ECHAM3.5 simulation is shown in Fig.1, upper and bottom panels respectively. At the equinox, the hemispheric symmetry in solar radiative forcing would imply a zonal mean temperature distribution approximately symmetric about the equator. However, other factors, such as orography and land-sea distribution generate asymmetries in the large scale circulation of the atmosphere, especially at middle and high latitudes (see for instance Fels et al. 1980, Andrews et al. 1983, and Manzini, 1994 for inter-hemispheric differences arising in integrations performed with annual mean solar radiative forcing). In addition, the 3-month MAM average may include asymmetries arising from different time scales associated with the boreal spring warming and the austral autumn cooling of the polar lower stratosphere.

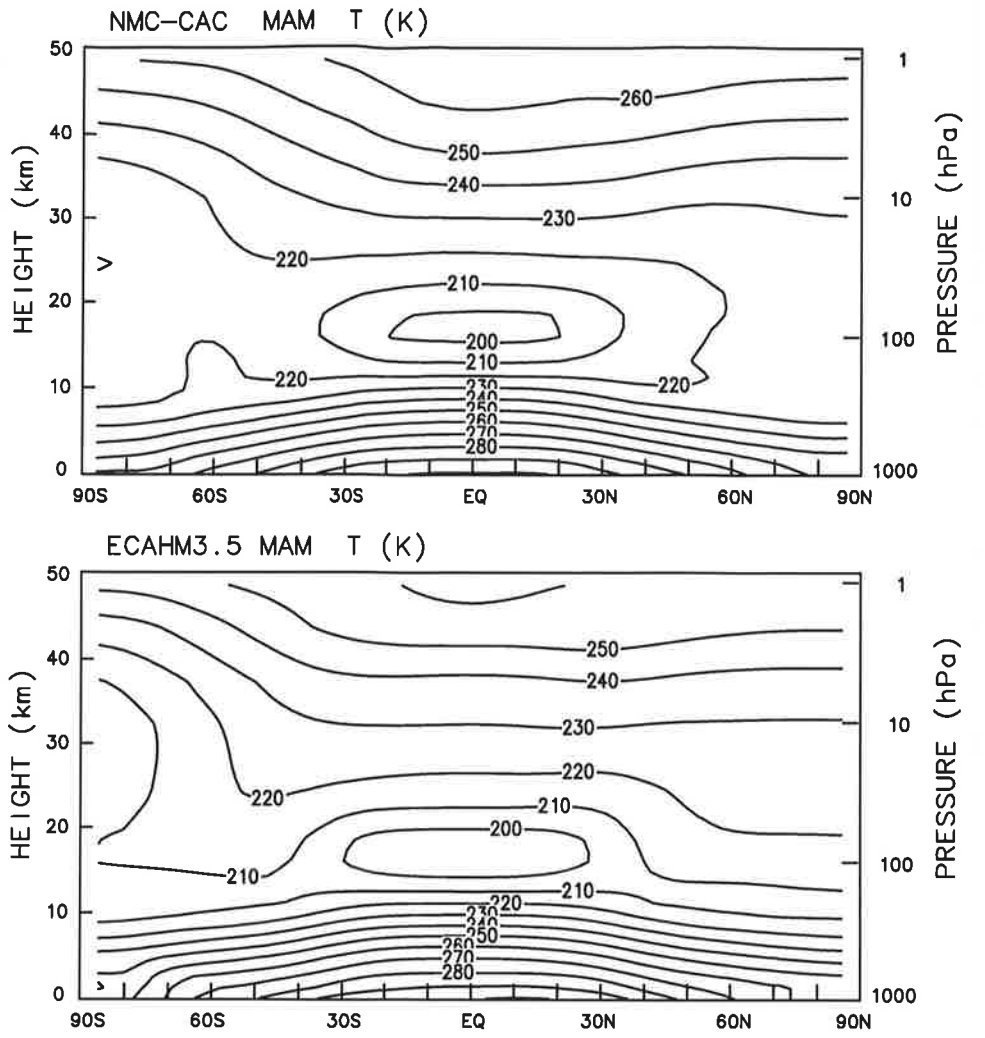

Figure 1 MAM time average zonal mean temperature from the 12-year NMC-CAC observations (upper panel) and from the 20-year ECHAM3.5 simulation (lower panel). Contour: 10° K.

As expected, Fig.1 shows that in the tropical atmosphere both the NMC-CAC and ECHAM3.5 zonal mean temperature fields are roughly symmetric about the equator. The observed and simulated zonal mean temperature are in good agreement in the troposphere, except for a cold bias (about 10°K) in the model at middle and high latitudes in the upper troposphere. This bias was also found for the DJF zonal mean temperature and persists throughout all the annual cycle, as the following results for June-August and September-November will show.

The NMC-CAC data show that in the stratosphere the zonal mean temperature increases with height. At the Northern hemisphere it is no longer dominated by a polar temperature minimum, as in winter, indicating that on average the vortex breakdown has already taken place. In the Southern hemisphere the zonal mean temperature is characterized by

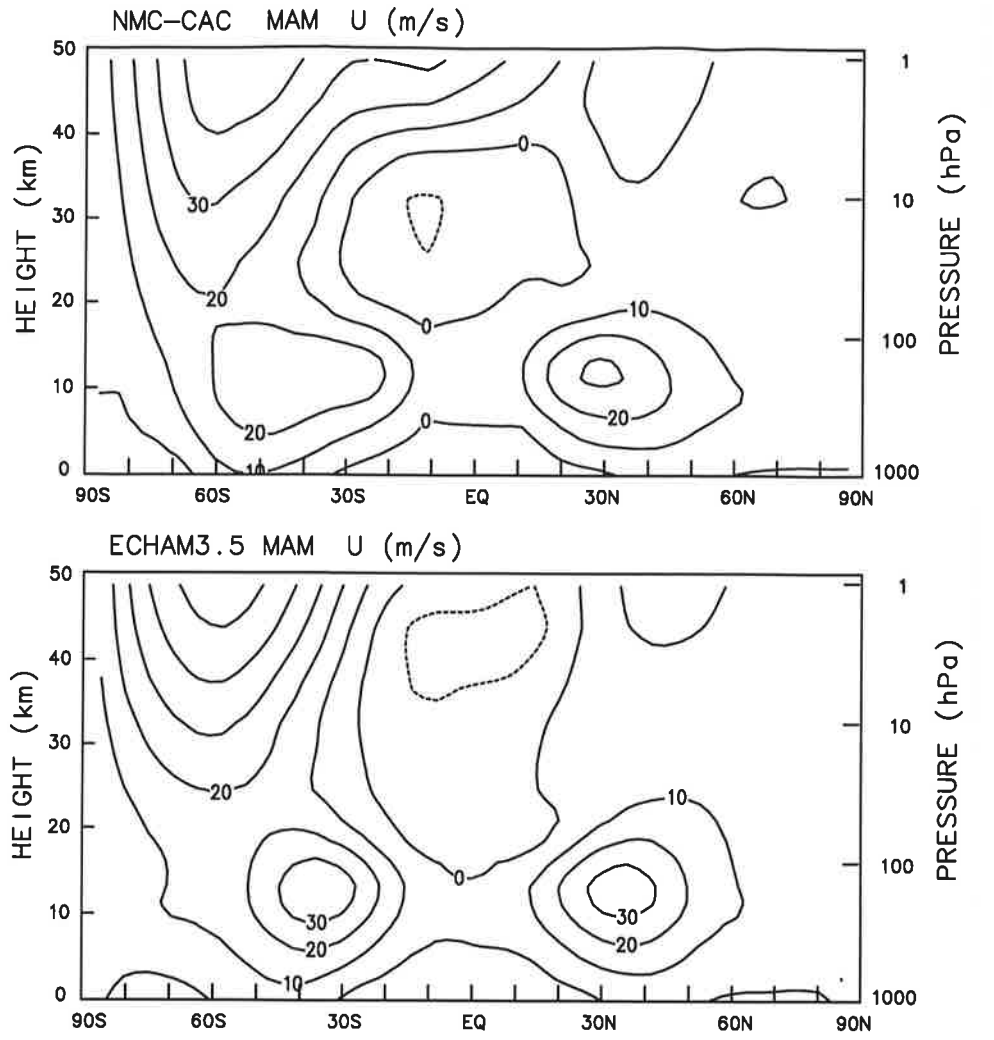

Figure 2 MAM time average zonal mean zonal wind from the 12-year NMC-CAC observations (upper panel) and from the 20-year ECHAM3.5 simulation (lower panel). Contour: 10 ms^{-1}.

a meridional temperature gradient at middle latitudes in the upper stratosphere. The temperature minimum at the South Pole in the lower stratosphere is strongly influenced by the situation in May, when the polar cooling is well under way.

The simulated mean temperature in the Northern hemisphere increases with height in good agreement with the analyzed observations, although the simulated temperature is slightly colder (about 5°K). This result suggests that on average the final stage of the Northern hemisphere vortex breakdown is well captured by the simulation, consistently with the realistic behavior of the simulation during February, see MB94. Preliminary results concerning the daily evolution of sudden stratospheric warming events spontaneously occurring in the ECHAM3.5 simulation also support this interpretation.

In the Southern hemisphere, the structure of the simulated mean temperature agrees with that observed. In addition, at middle latitudes in the upper stratosphere the meridional temperature gradient is reasonably realistic. This can also be seen from synoptic maps of the climatological monthly mean temperature (not shown), where it appears that the simulation of the reversal of the meridional temperature gradient evolves uniformly in longitude, in agreement with observations. However, at high latitudes in the middle stratosphere, the temperature minimum in the model is some 10°K too low. This bias indicates that the autumn polar cooling at the Southern hemisphere proceeds too quickly, thus accentuating the inter-hemispheric asymmetry in the model.

The MAM zonal mean zonal winds for the MAM for the 12 year NMC-CAC analyses and for the 20 year ECHAM3.5 simulation are shown in Fig.2. In the NMC-CAC dataset, the Southern hemisphere subtropical jet is much broader in latitude and somewhat weaker than the Northern hemisphere subtropical jet, the latter centered at about 30°N. This is not the case in the model, where the circulation in the troposphere is quite symmetric about the equator, with both jets located around 35°N and 35°S respectively. This difference between model and observations in the Southern hemisphere may be related to the low horizontal resolution currently used, presumably not sufficient to fully resolve the secondary westerly jet South of Australia.

In the Northern hemisphere stratosphere, both the observations and the model are dominated by very weak zonal mean winds, as expected by the very weak meridional gradient in zonal mean temperature. In the Southern hemisphere lower stratosphere the westerly winds are weak in both datasets, while in the upper stratosphere poleward of 50°S the simulated westerly winds are about 10 ms^{-1} too strong.

The mean westerly winds seen in the NMC-CAC data at the equatorial stratopause are the manifestation of the westerly phase of the semiannual oscillation in zonal wind (Reed, 1966; Hirota, 1980). It appears that the model fails to reproduce such an oscillation in the zonal wind, at least in its full strength, given that easterly winds dominate the equatorial upper stratosphere for MAM. Note however that weak westerly zonal mean winds are found in the simulation in May (not shown), although they are confined to the vicinity of the equatorial stratopause. A thorough investigation of the semiannual oscillation is not pursued in the current work.

The interannual variability of the zonal mean temperature for MAM from the 12 year NMC-CAC analyses is shown in Fig.3. The corresponding fields from the 20-year ECHAM3.5 simulation are shown in Fig.4.

In March (Fig.3, upper panel), the NMC-CAC dataset shows that the stratosphere is characterized by a marked increase in variability poleward of 60°N, roughly independent with height apart from an indication of two local polar maxima, respectively in the lower and upper stratosphere. In the upper troposphere at high latitudes, the variability sharply

increase with height. The interannual variability during March is associated with the irregular timing of the final warming leading to the summer circulation dominated by easterly winds. The pattern and the amount of the simulated variability in March (Fig.4, upper panel) are quite comparable to that observed. As shown in MB94 for late winter, in the Northern hemisphere the simulation in early spring appears to be realistic.

In April (Fig.3, middle panel), in the Northern hemisphere stratosphere, the NMC-CAC interannual variability is about half of that in March. Furthermore, in May (Fig.3, lower panel) the variability is basically negligible. It must be recalled that some of the NMC-CAC variability in the upper stratosphere (about few degrees) is caused by changes in data acquisition (see Randel, 1992 and Finger et al. 1993). Although, this bias should not greatly affect the shape of the variability distribution, it is presumably responsible for part of the variability seen in the tropical upper stratosphere during MAM. Randel (1992) suggests to look at the variability in the mean zonal wind, that is not a strong function of horizontal position and therefore it is less affected by the data acquisition problem. In addition, note that the large interannual temperature variability over Antarctica in the NMC-CAC data is an artifact of a change in the NMC tropospheric analyses (Randel, 1992).

In the model, the interannual variability also decreases from March to April (Fig.4, upper and middle panels), but mainly in the lower stratosphere. Synoptic maps of individual monthly mean temperature fields (not shown) suggest that the simulated variability maximum in the upper stratosphere in April is associated with a large scale circulation still dominated by planetary waves. In the lower stratosphere, the synoptic maps indicate that by April the warmest temperature already occur at high latitudes, in both observations and simulation, hence the interannual variability is low.

A month later, in May (Fig.4, lower panel), the variability is reduced to a few degrees only. Note that the interannual variability in over Antarctica and in the tropical upper stratosphere is negligible for the ECHAM3.5 simulation, supporting the spurious origin of the variability found in the NMC-CAC data.

The interannual variability of the zonal mean zonal wind for MAM from the 12 year NMC-CAC analyses is shown in Fig.5. The corresponding fields from the 20-year ECHAM3.5 simulation are shown in Fig.6.

In March (Fig.5, upper panel), the NMC-CAC variability in the middle-high latitudes of the Northern hemisphere is characterized by two maxima of about equal amplitude, one just below 10 hPa around 75°N, and the other centered at 1 hPa and 50°N. The pattern of the March variability is therefore rather different from that in February (see MB94 Fig.10, lower panel), dominated by a single variability maximum between 60°N and 70°N. In the model (Fig.6, upper panel) most of the variability is still located in the middle-upper stratosphere at about 70°N, as in February (see MB94 Fig.11, lower

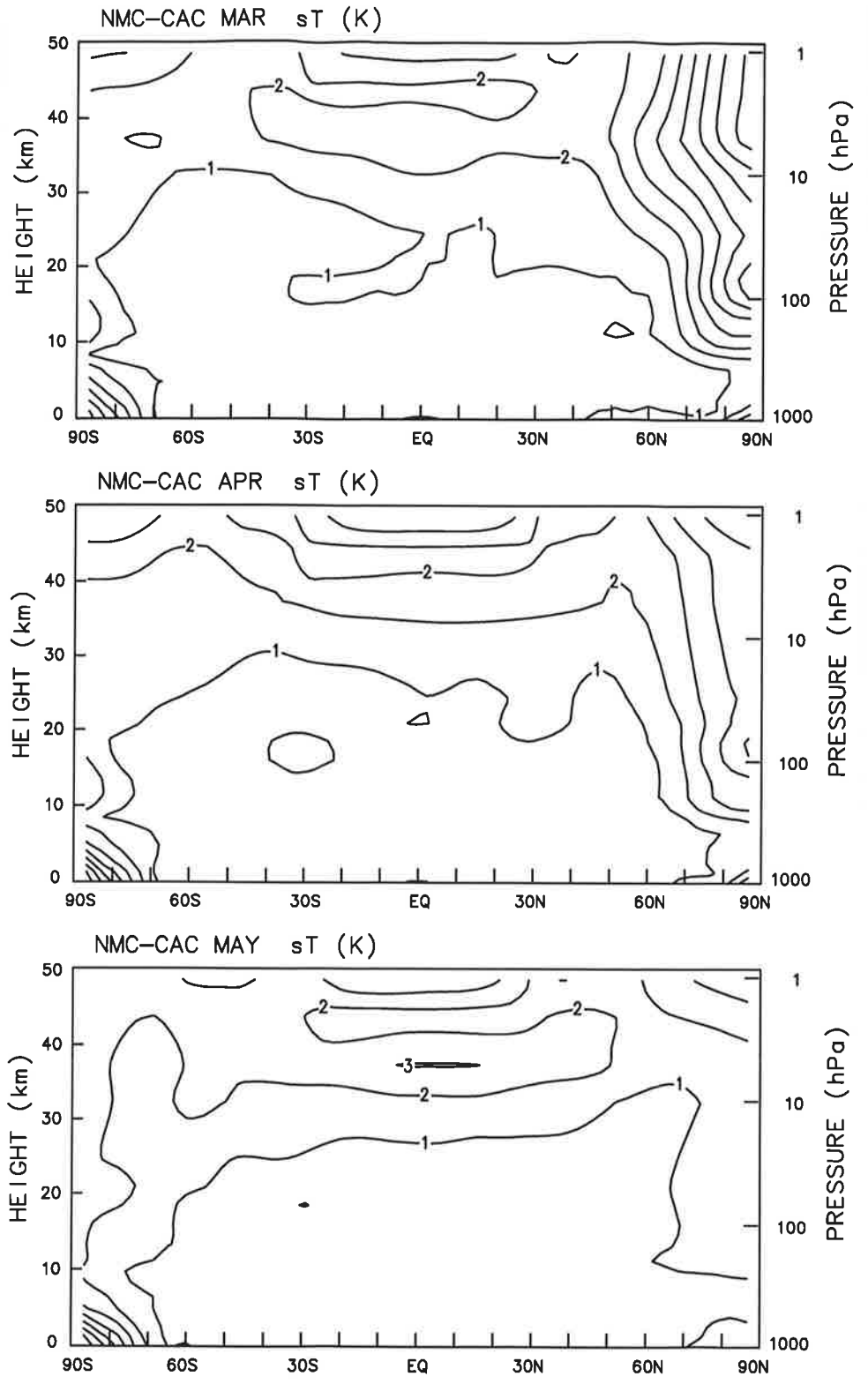

Figure 3 Monthly interannual variability (standard deviation) of the zonal mean temperature from the 12-year NMC-CAC observations for March (upper panel), April (middle panel), and May (bottom panel). Contour: 1° K.

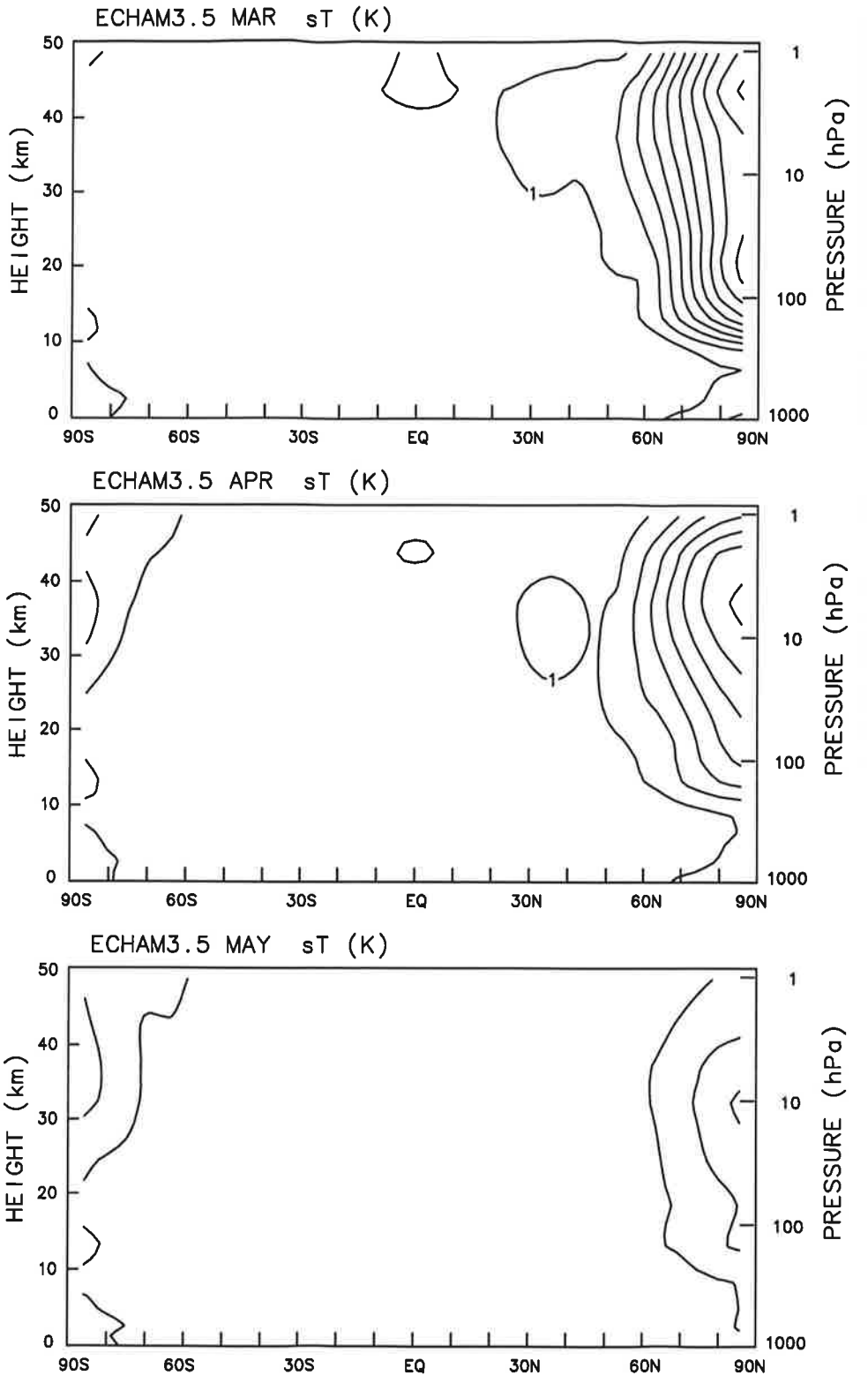

Figure 4 Monthly interannual variability (standard deviation) of the zonal mean temperature from the 20-year ECHAM3.5 simulation for March (upper panel), April (middle panel), and May (bottom panel). Contour: 1° K.

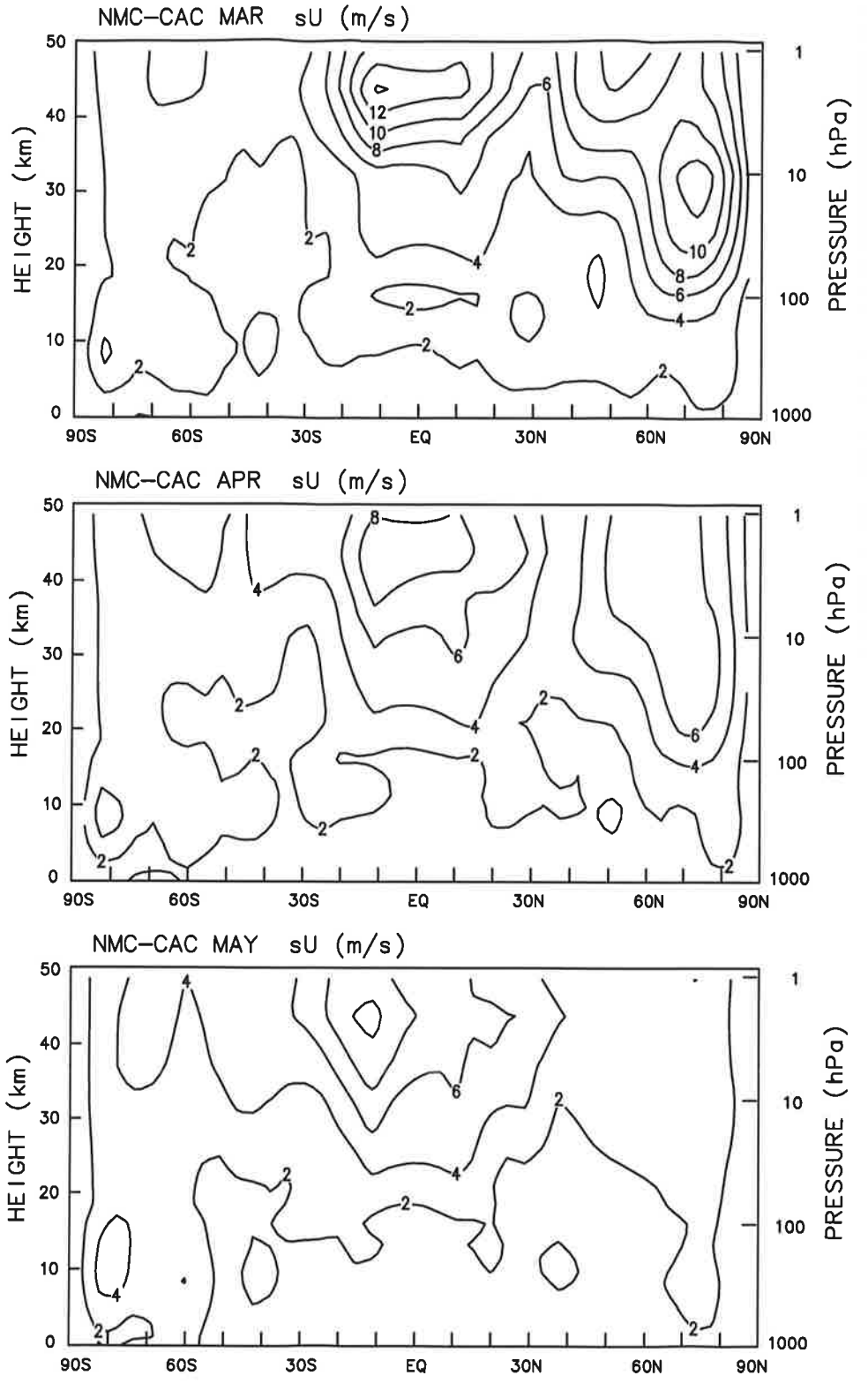

Figure 5 Monthly interannual variability (standard deviation) of the zonal mean zonal wind from the 12-year NMC-CAC observations for March (upper panel), April (middle panel), and May (bottom panel). Contour: 2 ms^{-1}.

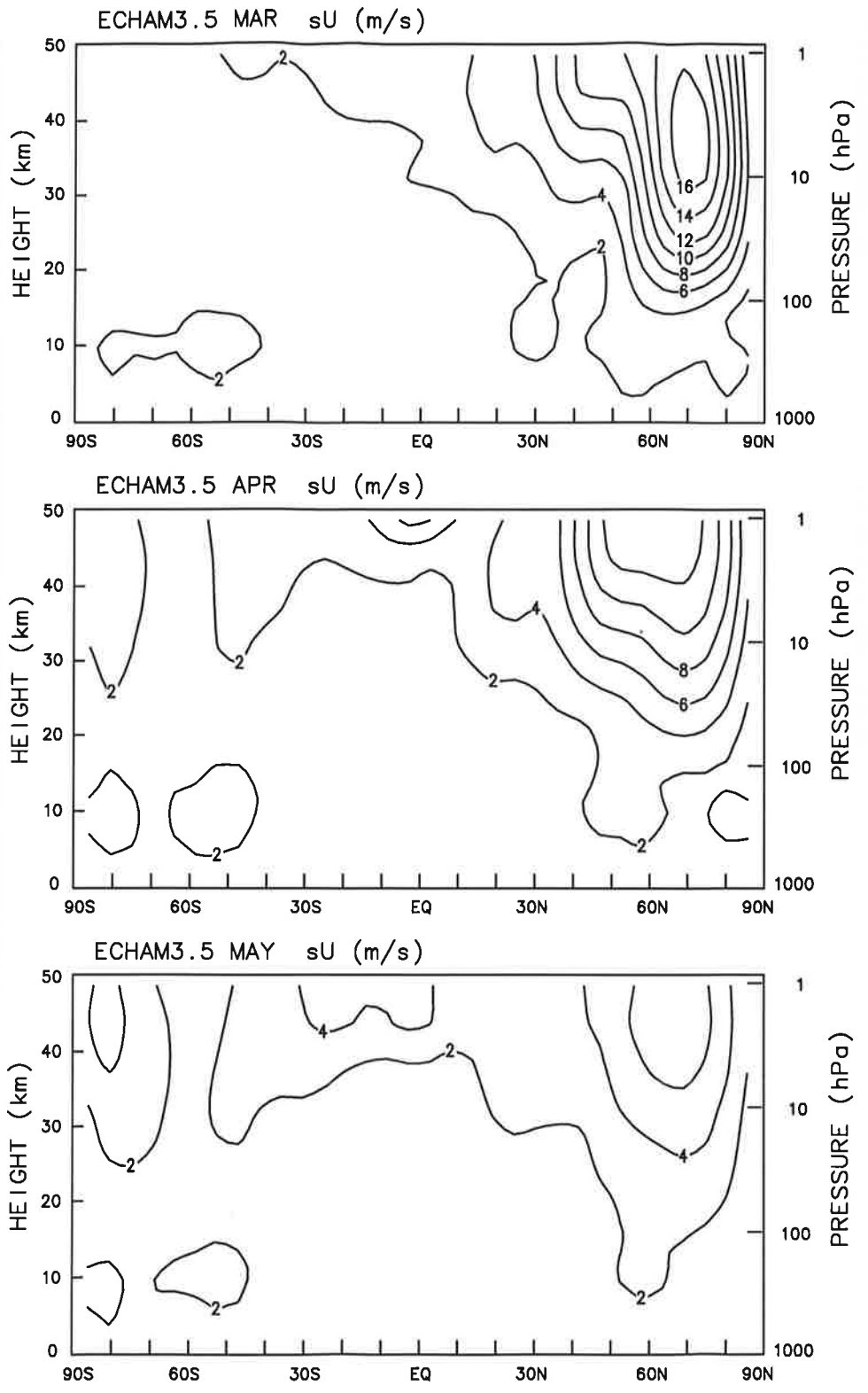

Figure 6 Monthly interannual variability (standard deviation) of the zonal mean zonal wind from the 20-year ECHAM3.5 simulation for March (upper panel), April (middle panel), and May (bottom panel). Contour: 2 ms^{-1}.

panel). It may be that the upper stratospheric variability maximum is not captured by the model because of insufficient vertical resolution in the mesosphere. Alternatively, the simulation may present a slight excess of planetary wave activity in the middle stratosphere, as found for instance in January (see MB94).

The variability maximum (stronger in March, Fig.5, upper panel) seen in the NMC-CAC data just below the equatorial stratopause is indicative of changes in the timing of the westerly phase of the semiannual oscillation. This would explain the insignificant variability at the equatorial stratopause in the model (Fig.6), given the weakness of the westerly phase of such oscillation in the simulation.

In April (Fig.5, middle panel), in the Northern hemisphere, the NMC-CAC variability maximum is strongly reduced with respect to that in March, as expected from the zonal mean temperature variability. The simulated variability (Fig.6, middle panel) also decreases, but at a somewhat slower rate. In May (Fig.5 and Fig.6, lower panels) the variability is quite low in both datasets.

3. The June - August period

The JJA zonal mean temperature for the 12 year NMC-CAC analyses and for the 20 year ECHAM3.5 simulation is shown in Fig.7. The polar lower stratosphere is know to be colder during the austral winter than during the boreal winter (Barnett and Corney, 1985; Mechoso et al., 1985). A comparison of the current Fig.7 with MB94 Fig.6 (upper panel) shows indeed that the NMC-CAC zonal mean temperature is as low as 190°K at the South Pole between 20-25 km during JJA, while reaching only about 210°K at the North Pole in the lower stratosphere during DJF. It is now generally recognized that a weaker polar vortex and warmer temperatures during the boreal winter are ultimately connected to the activity of the tropospheric planetary waves, which in turn are more favourably forced by the orography and the land-sea distribution of the Northern hemisphere.

As shown by the NMC-CAC dataset, also in the ECHAM3.5 model the polar lower stratosphere is colder during the austral than the boreal winter. A difference of about 20°K (compare to MB94 Fig.6, lower panel) is found between the austral and boreal polar minimum temperature in the model, in agreement with that suggested by the analyzed observations. Given the tendency of general circulation models (without gravity wave drag parametrization) to produce extremely low temperature during the antarctic polar night (simulated temperature more than 20-30°K colder than observed, see for instance Hamilton et al. 1995), it is interesting that in the current ECHAM3.5 model the austral winter cold bias is limited to about 10-20°K. As found in MAM, the cold bias in the model in the stratosphere is mainly confined to the high latitudes, poleward of about 60°S. The vertical extent of the polar temperature minimum is also relatively confined, given that above 10 hPa the isotherms are turning horizontal at high

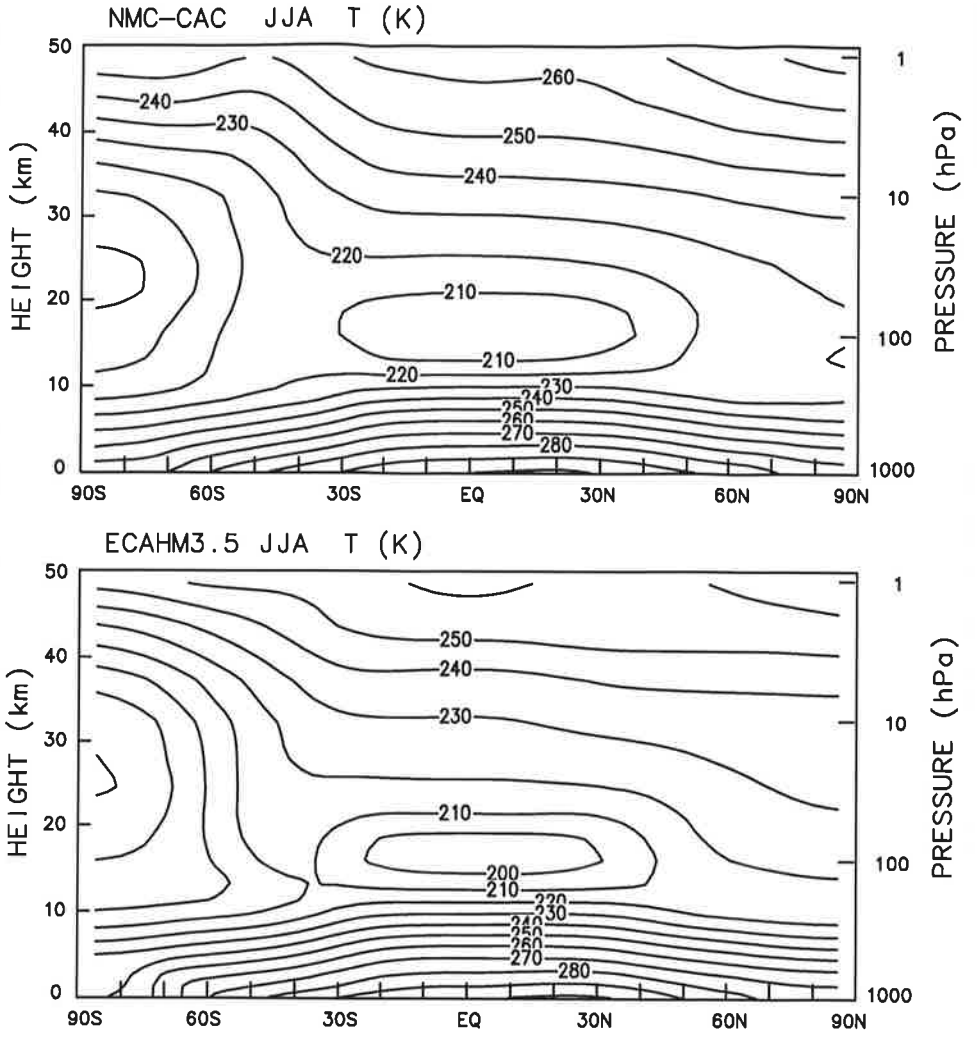

Figure 7 JJA time average zonal mean temperature from the 12-year NMC-CAC observations (upper panel) and from the 20-year ECHAM3.5 simulation (lower panel). Contour: 10^{o} K.

latitudes and that the middle latitude meridional temperature gradient is reasonably well simulated. The relative success of the current simulation appears to be a direct consequence of the downward influence of the Rayleigh friction applied in the mesosphere. Short trial simulations with a substantially reduced damping coefficient of the mesospheric drag were indeed characterized by a more pronounced cold bias.

In the Northern hemisphere stratosphere, the zonal mean temperature increases with height, in reasonable agreement with observations. However, the zonal mean temperature maximum at the stratopause at the North Pole is underestimated in the model, similarly to the behavior at the South Pole during the DJF season.

In the troposphere, the model still shows a cold bias at the tropopause at middle-high

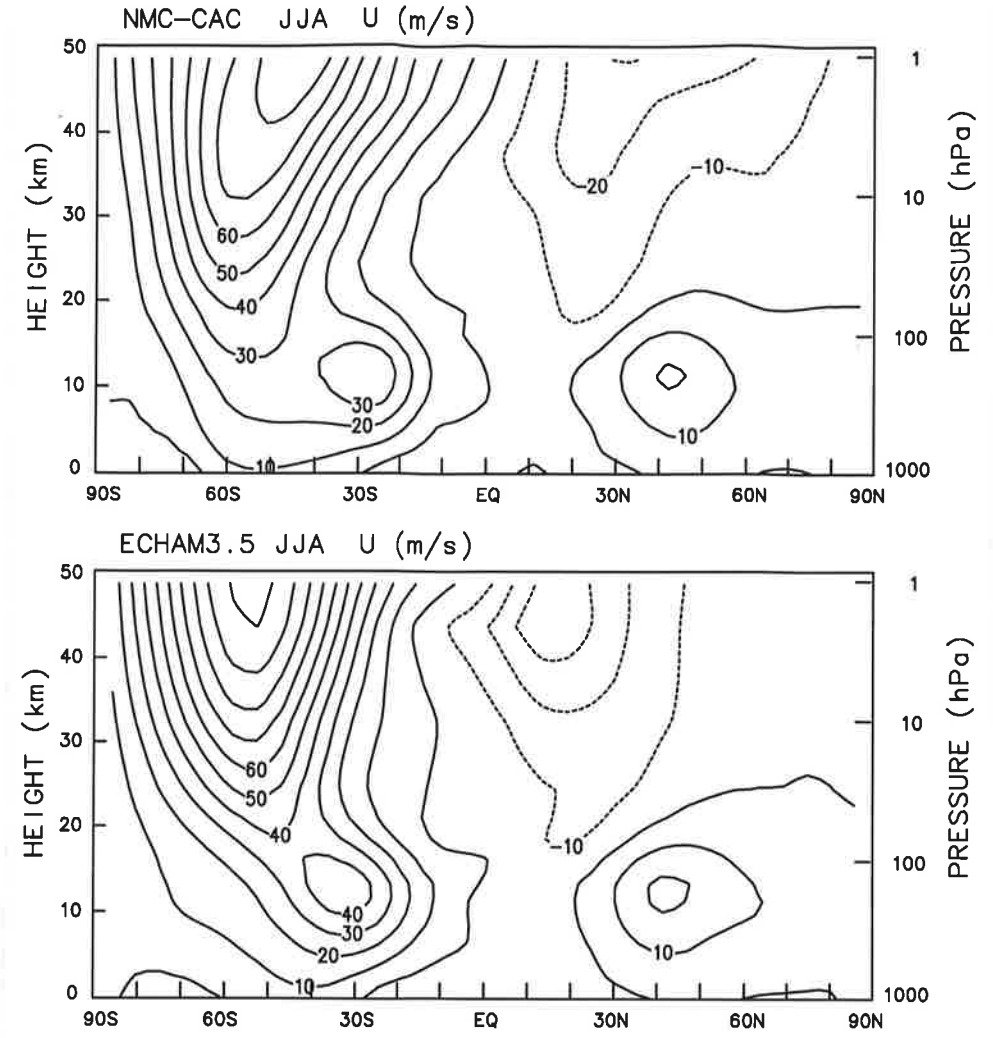

Figure 8 JJA time average zonal mean zonal wind from the 12-year NMC-CAC observations (upper panel) and from the 20-year ECHAM3.5 simulation (lower panel). Contour: 10 ms^{-1}.

latitudes, as pointed out in the previous section and in MB94. At the surface over Antarctica, the ECHAM3.5 model is too cold. Note that the simulated zonal mean temperature is actually more in agreement with ECMWF analyses (see Roeckner at al. 1992). This discrepancy between NMC and ECMWF analyses was already noted by Randel (1988), among others.

The JJA zonal mean zonal wind for the 12 year NMC-CAC analyses and for the 20 year ECHAM3.5 simulation is shown in Fig.8. In the Northern hemisphere troposphere, the strength and the location of the simulated and observed summer westerly jet are comparable. In the Southern hemisphere instead, the simulated westerly winter jet is somewhat too strong at 30°S and too weak poleward of 50°S. This result suggests that the secondary westerly jet occurring South of Australia is not well represented in the

current low resolution model. Comparisons of the climatological average of the zonal mean wind during JJA in the Southern Hemisphere at T21 and T42 horizontal truncations performed with the ECHAM3 model have shown that the JJA winter tropospheric jet becomes realistically broad only at T42 (Roeckner et al. 1992).

In agreement with the relatively modest magnitude of the cold bias in the Southern hemisphere, the simulated zonal mean winds are of reasonable strength in the lower stratosphere, and the subtropical and westerly jets are clearly separated. Also the location of the stratospheric jet core in the lower stratosphere (around 55°N) is well captured by the simulation. In the upper stratosphere the behavior of the simulation is not so satisfactory: The westerly jet does not tilt equatorward with height and its magnitude increases with height at a faster rate, reaching 100 ms^{-1} at the stratopause (instead of 80 ms^{-1}, as in the NMC-CAC data). The westerly wind bias is mainly a contribution to the JJA seasonal average coming from August.

The summer hemisphere is dominated by weak easterly winds that increase with height and are largest in the tropical stratosphere, in both observations and simulation.

In both the NMC-CAC and ECHAM3.5 datasets the JJA winter variability in zonal mean temperature is at most few degrees and is confined to the upper stratosphere around 50°S-60°S. Therefore only the interannual variability in zonal mean zonal wind (presumably more reliable) is shown, in Fig.9 for the 12 year NMC-CAC analyses and in Fig.10 for the 20-year ECHAM3.5 simulation.

In June (Fig.9, upper panel), the major feature in the NMC-CAC data is a variability maximum of more than 12 ms^{-1}, centered in the upper stratosphere at about 20°S. During July and August (Fig.9, middle and lower panel respectively) such region of enhanced variability is seen to increase in magnitude, move poleward and extend slightly downward. In August it has reached 40°S and 16 ms^{-1}. This region of enhanced variability appears to be associated with the poleward and downward movement of the stratospheric vortex, usually a rapid and abrupt change taking place at any time during the JJA winter season. This behavior was first noted by Mechoso et al. (1985), who studied the first four years of the NMC-CAC dataset used here. When the poleward and downward shift occurs early in the JJA winter, the August zonal wind is characterized by a closed jet core (as in the climatology). Occasionally the shift can take place in late August instead, allowing for strong westerly wind in the upper stratosphere in the August mean.

Fig. 9 also show that two secondary variability maxima, one at high latitudes, about 70°S, and the other centered at about 10°N, occur in the upper stratosphere during June and the following months. The maximum at 10°N, presumably related to the semiannual oscillation, is also strengthening from June to August.

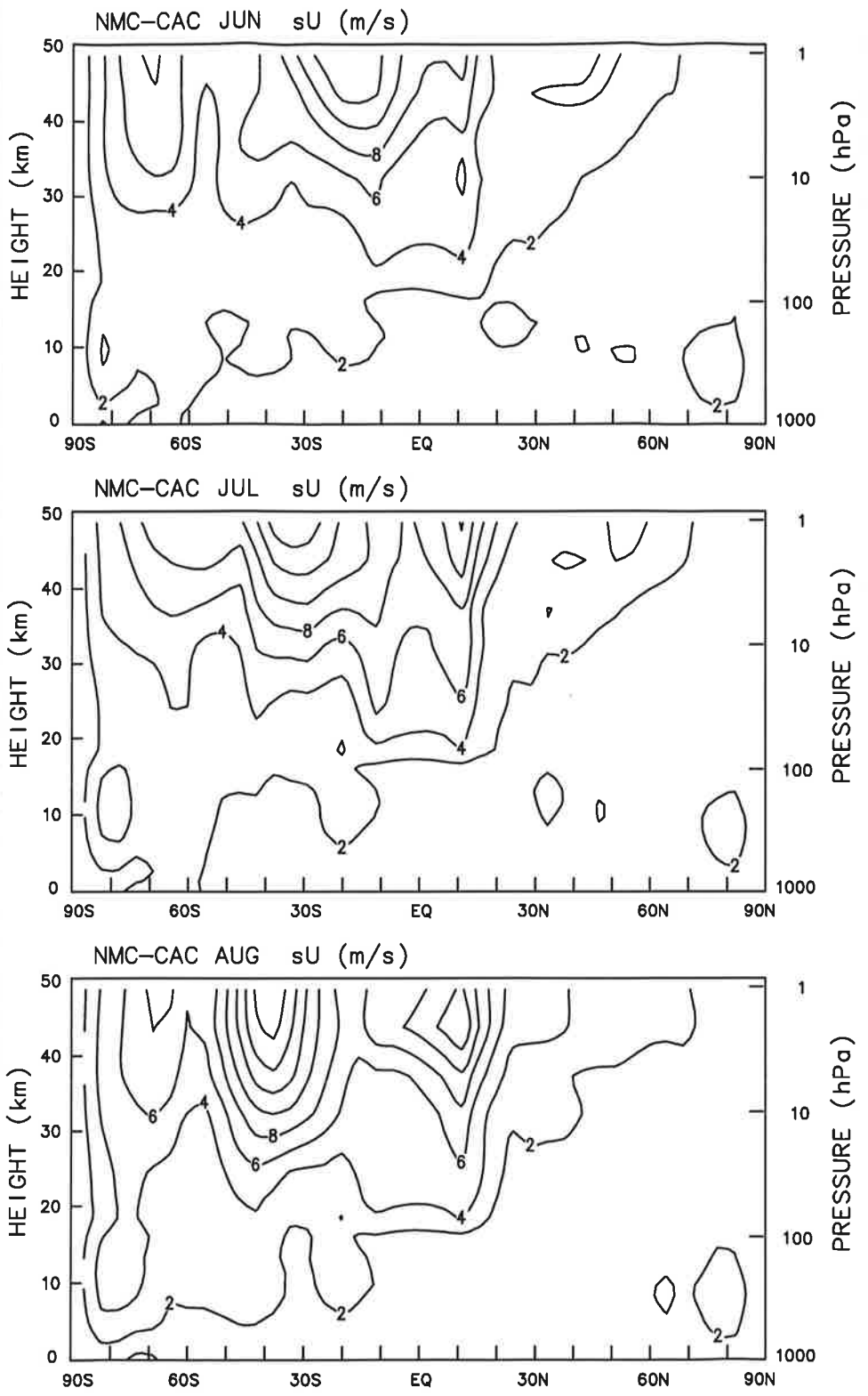

Figure 9 Monthly interannual variability (standard deviation) of the zonal mean zonal wind from the 12-year NMC-CAC observations for June (upper panel), July (middle panel), and August (bottom panel). Contour: 2 ms^{-1}.

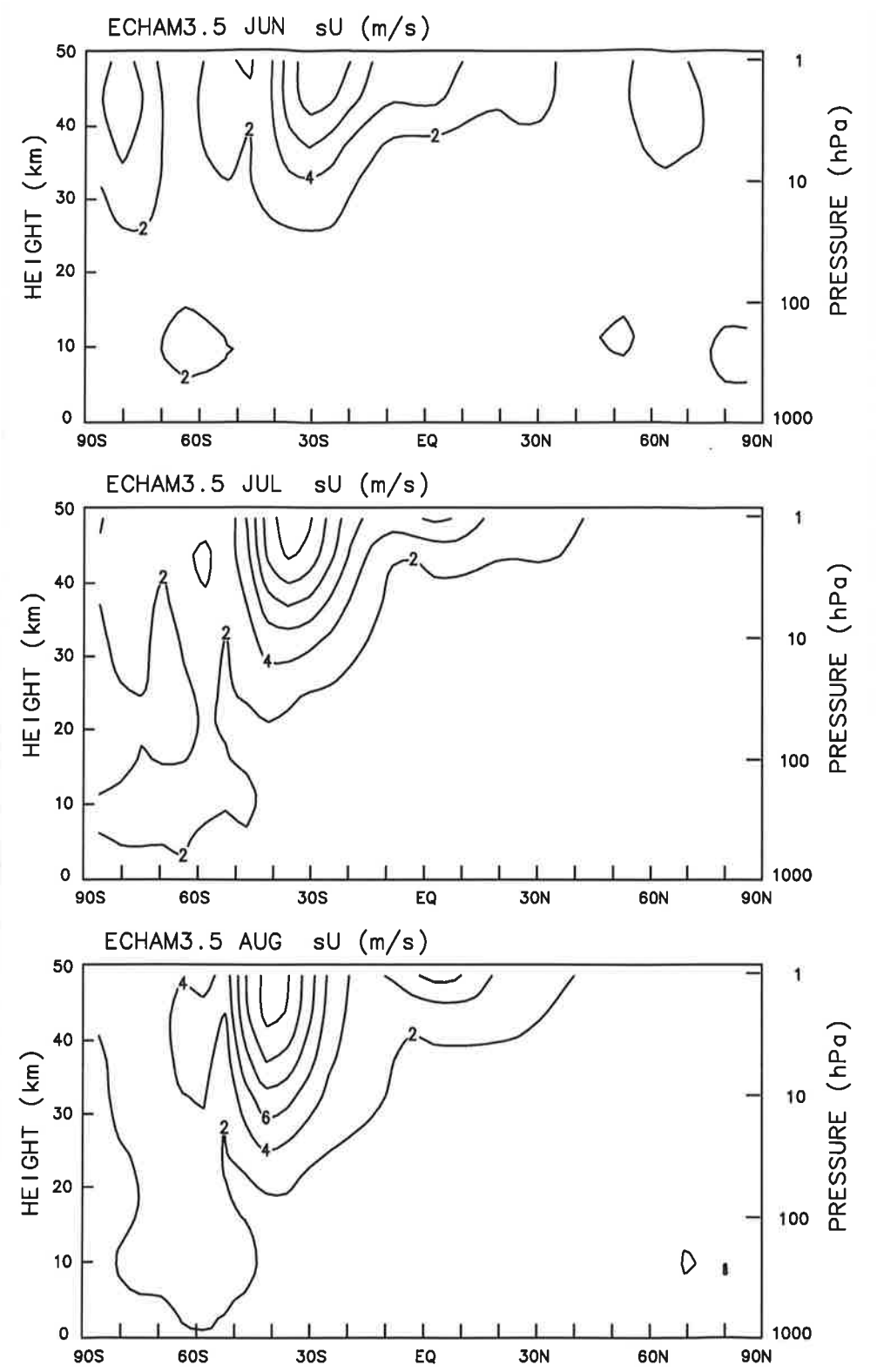

Figure 10 Monthly interannual variability (standard deviation) of the zonal mean zonal wind from the 20-year ECHAM3.5 simulation for June (upper panel), July (middle panel), and August (bottom panel). Contour: 2 ms^{-1}.

In comparison with the DJF winter, the variability during the JJA winter is substantially smaller at high latitudes and in the lower stratosphere. The major peak of variability in August, centered at 40°S and 1 hPa, is instead comparable to values found for the DJF winter months. This is probably a consequence of the very strong winds in the upper stratosphere in August.

Fig.10 shows that the model reproduces the subtropical region of high variability in zonal mean wind and that this variability maximum moves poleward and extends downward from June to August. The high latitude maximum is however virtually missing in the model, and the other maximum centered at 10°N is only slightly developed. Although the variability maximum increases from June to August, its value always remains below that indicated by the NMC-CAC analyzed observations. Moreover, in August the simulated monthly mean, zonal mean jet does not close off in the upper stratosphere, for any of the 20 years available from the integration (not shown).

4. The September - October period

The SON zonal mean temperature for the 12 year NMC-CAC analyses and for the 20 year ECHAM3.5 simulation is shown in Fig.11. In the Southern hemisphere, the NMC-CAC data show that the stratosphere is warmest at the South Pole stratopause. In addition, a clearly defined temperature minimum (about 210°K) is still present in the lower stratosphere and a minor temperature minimum is found in the upper stratosphere at about 50°S. The presence of the polar temperature minimum in the lower stratosphere indicates that on average the polar vortex breakdown is still under way during the austral spring. The transition to summer easterly therefore appears to be delayed with respect to that in the Northern hemisphere, where the MAM average showed that the polar minimum already disappeared in spring (see Fig.1). In the Northern hemisphere, the lower stratosphere cooling is already progressing, as shown by the midlatitude upper stratosphere meridional temperature gradient. In this latter case, the zonal mean temperature fields of the austral and boreal autumn hemisphere resemble each others (compare with Fig.1).

In the ECHAM3.5 model the zonal mean temperature distribution presents an even more pronounced zonal mean temperature minimum in the Southern hemisphere lower stratosphere. The cold bias also extends into the middle and upper stratosphere. In addition, the secondary minimum in the upper stratosphere at 50°S is missing in the model. This discrepancy is particularly severe in September and October (not shown). In the Northern hemisphere, the polar stratosphere is about 10°K colder in the model, a bias comparable to that found for the austral autumn. Although the polar bias has already developed in the Northern hemisphere, synoptic maps of the monthly mean temperature at 50 hPa (not shown) indicate that quasi-stationary planetary waves are beginning to

develop in the model, in agreement with the analyzed observations.

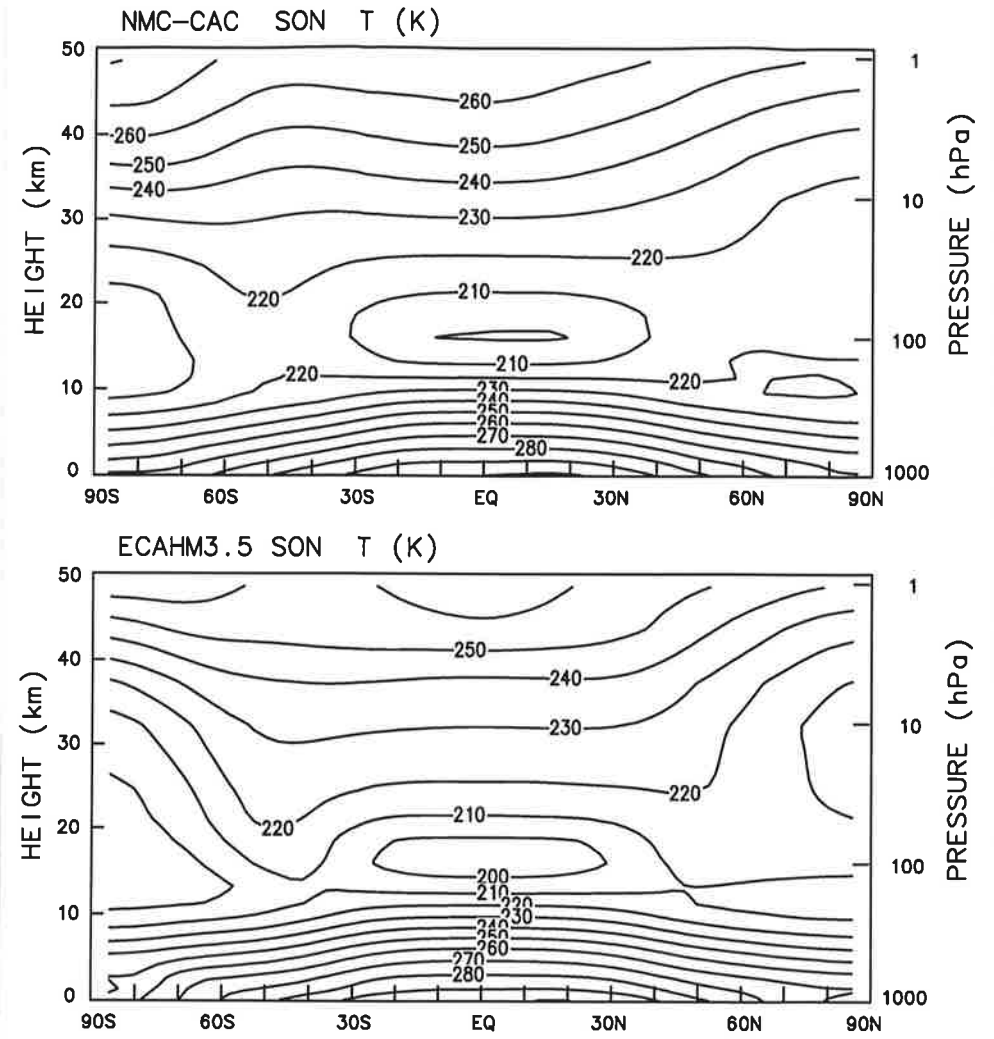

Figure 11 SON time average zonal mean temperature from the 12-year NMC-CAC observations (upper panel) and from the 20-year ECHAM3.5 simulation (lower panel). Contour: 10° K.

The SON zonal mean zonal wind for the 12 year NMC-CAC analyses and for the 20 year ECHAM3.5 simulation is shown in Fig.12. In the Southern hemisphere the NMC-CAC dataset is characterized by a westerly closed jet with the core in the middle stratosphere. Weak westerly winds therefore dominate the upper and lower stratosphere. The closure of the jet is expected by the structure of the zonal mean temperature in the upper stratosphere, with the warmest temperature at the South Pole. In the ECHAM3.5 model, the Southern hemisphere westerly jet is too strong (about 30% more). Most importantly, the simulated jet does not close off. The simulated westerly winds are somewhat too strong also in the Northern hemisphere. Note that the westerly wind bias is stronger for the boreal than austral autumn (compare with Fig.2). The occurrence in the simulation

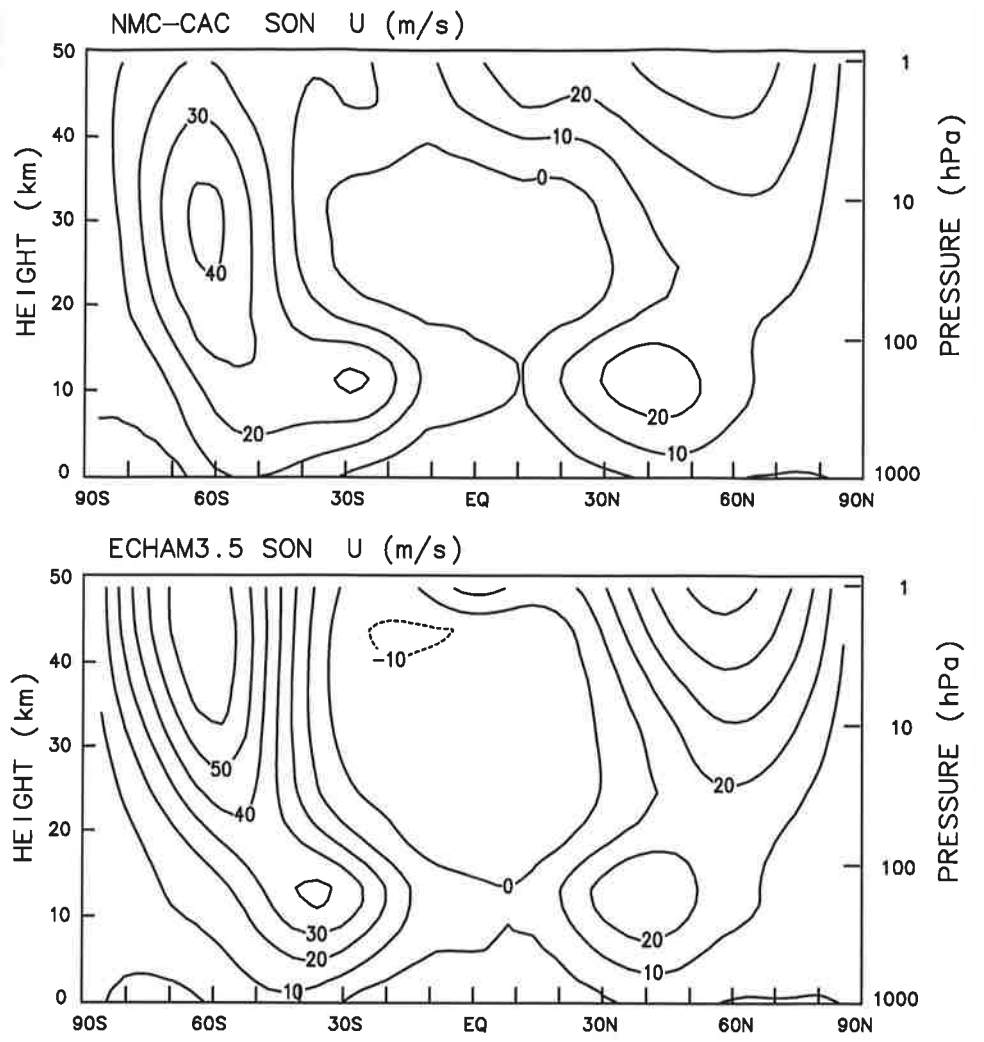

Figure 12 SON time average zonal mean zonal wind from the 12-year NMC-CAC observations (upper panel) and from the 20-year ECHAM3.5 simulation (lower panel). Contour: 10 ms^{-1}.

of weak westerly winds at the equatorial stratopause is suggestive of a tentative westerly phase of the semiannual oscillation during SON.

That a substantial discrepancy exists between the model and the analyzed observations during the austral spring is also illustrated by the climatological October temperature at 50 hPa, shown in Fig.13 for the 12-year NMC-CAC dataset and for the 20 year ECHAM3.5 simulation, respectively. In the observations, a quasi-stationary planetary wavenumber one dominates the large scale temperature field, characterized by warm air South of Australia and cold air just off the South Pole, at about 30°W. Evidence of quasi-stationary planetary waves in the Southern hemisphere during spring was also found by Randel (1988), who studied the first 8 years of the current NMC-CAC dataset. The simulated temperature field is instead virtually zonally symmetric, with the cold air

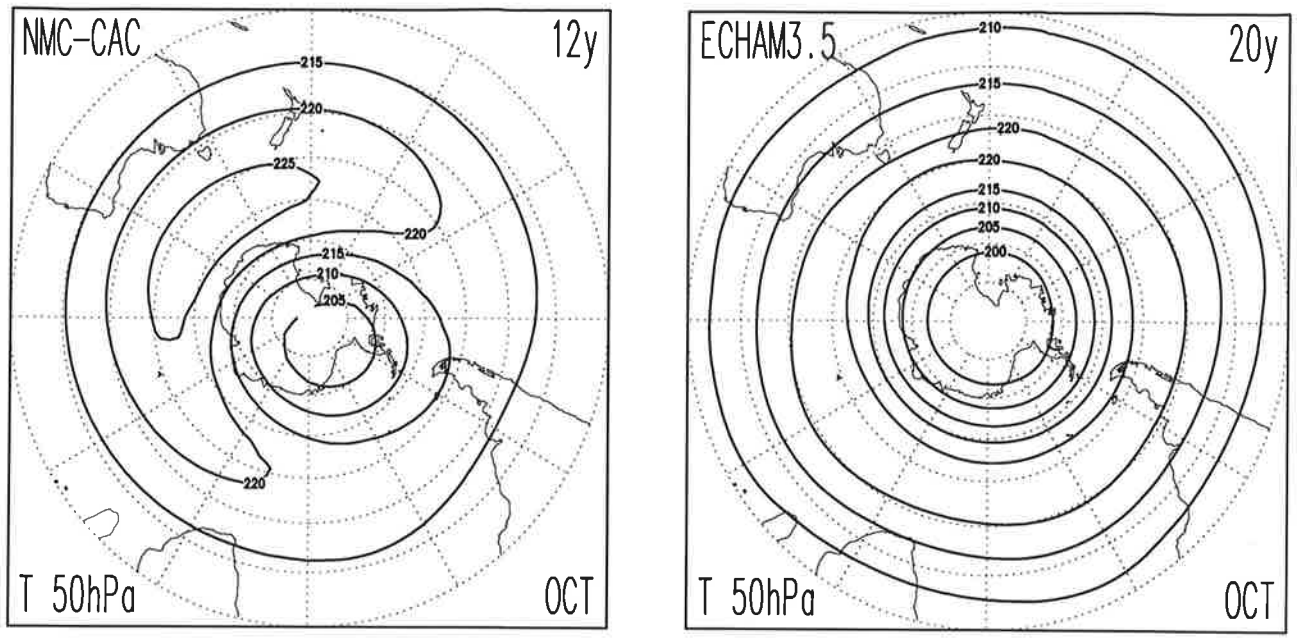

Figure 13 Southern hemisphere October mean temperature at 50 hPa from the 12-year NMC-CAC observations (at left) and from the 20-year ECHAM3.5 simulation (at right). Contour: 5° K.

located over the South Pole and no indications of any substantial planetary wave activity.

It is speculated that this model deficiency is caused by insufficient horizontal resolution. More precisely, the T21 truncation may not be able to simulate the generation of planetary waves by the Antarctic continent. Some evidence of the importance of the Antarctic continent in determining zonal asymmetries in the large scale circulation of the Southern hemisphere was presented by James (1988), with a simple barotropic model. Although the lack of a tropospheric forcing is presumably the major cause of the discrepancy, other factors may aggravate it. For instance, the unrealistic zonal mean circulation at the beginning of the austral spring and a general lack of small scale dynamical forcing in the ECHAM3.5 model may substantially contribute to the model bias.

As for JJA, only the interannual variability of the zonal mean zonal wind is shown for SON, in Fig. 14 and Fig.15, respectively from the 12 year NMC-CAC dataset and the 20-year ECHAM3.5 simulation.

The NMC-CAC dataset show that in September (Fig.14, upper panel), the August subtropical region of high variability in the Southern hemisphere has virtually

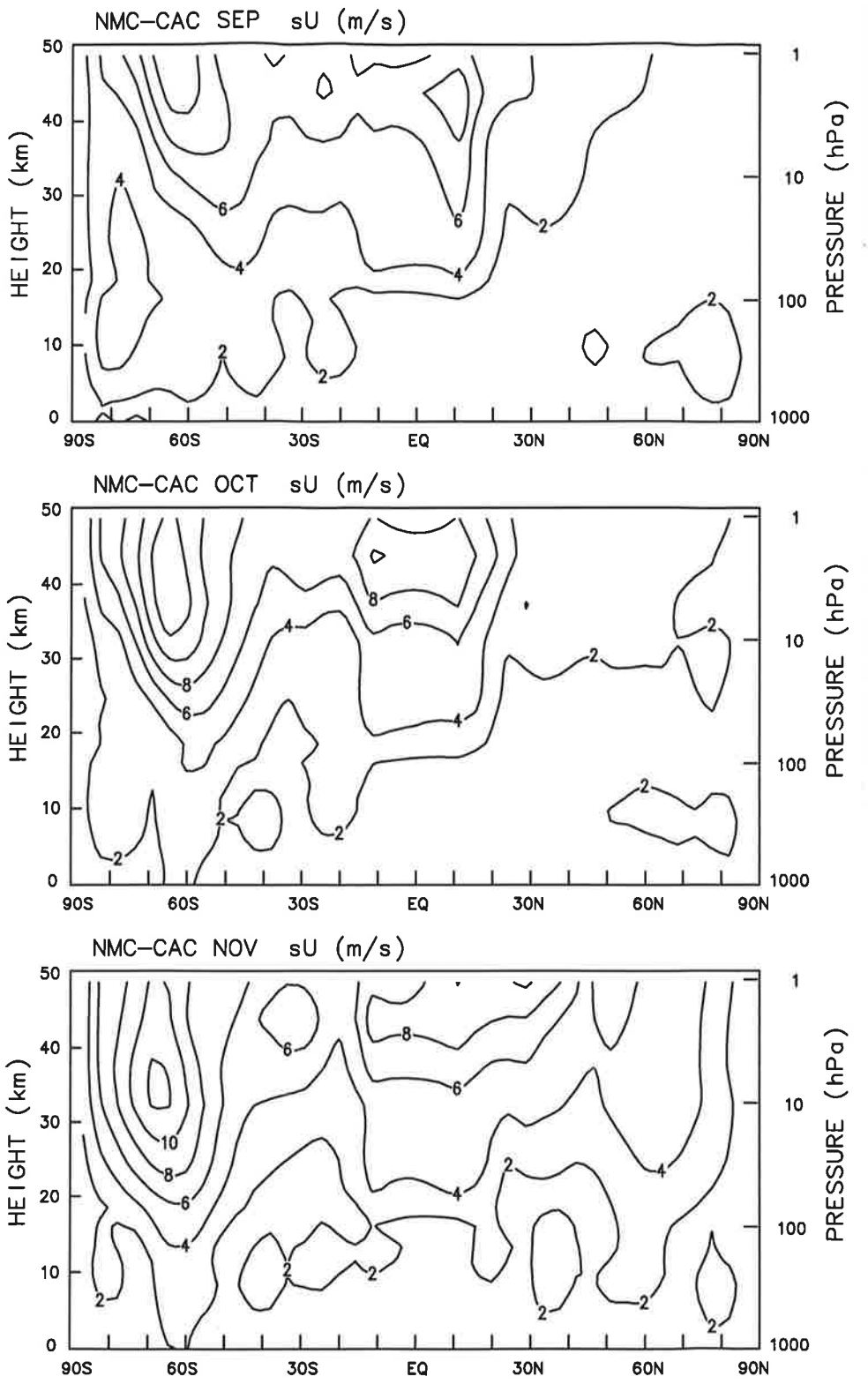

Figure 14 Monthly interannual variability (standard deviation) of the zonal mean zonal wind from the 12-year NMC-CAC observations for September (upper panel), October (middle panel), and November (bottom panel). Contour: 2 ms^{-1}.

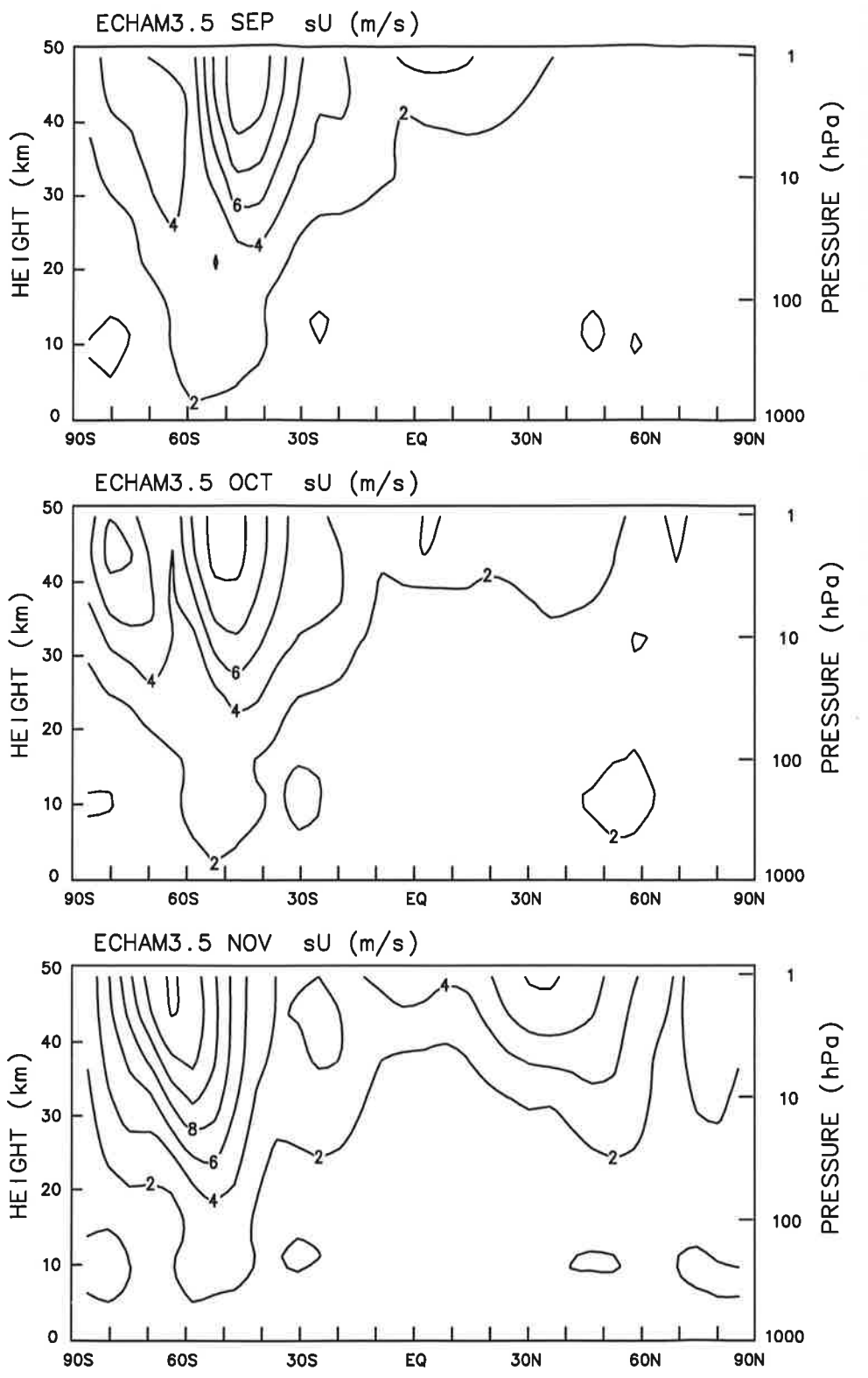

Figure 15 Monthly interannual variability (standard deviation) of the zonal mean zonal wind from the 20-year ECHAM3.5 simulation for September (upper panel), October (middle panel), and November (bottom panel). Contour: 2 ms^{-1}.

disappeared (Fig.9, lower panel). The September variability is substantially smaller than in August and is mainly confined to the high latitude upper stratosphere. This feature confirms the suggestion of Mechoso et al. (1985) that the poleward and downward movement of the stratospheric westerly jet during JJA reaches more or less always the same position and magnitude in September.

In October and November (Fig.14, middle and bottom panels), the high latitude zonal mean zonal wind variability is seen to increase and extend to the lower stratosphere in the Southern hemisphere. The October variability is presumably associated with interannual variations in the forcing and vertical propagation of the quasi-stationary planetary waves seen in Fig.13 (left panel). In November the variability is highest in the middle stratosphere at about 65°S.

Given the discrepancy in the climatological state between model and analyzed observations, it not surprising that the simulated variability during SON in the Southern hemisphere (Fig.15) is qualitatively different from that observed. The maximum in September is comparable to that of August (instead than substantially less) and is located about 20° equatorward of that observed. In October the simulated variability presents two maxima in the Southern hemisphere, and a minimum where the NMC-CAC variability is largest (at about 65°S, upper stratosphere). Most of the variability remains confined to the upper and middle stratosphere even in November. It appears that the lack of eddy activity in the model results in a stratospheric jet decreasing in magnitude more or less in place, instead of moving poleward and downward from September to November.

5 Conclusions

The stratospheric climate and variability of a 20-year integration performed with the ECHAM3.5 general circulation model has been studied. The results for the December-February period were presented in Part I (MB94), while the current Part II dealt with the remaining part of the year. The ECHAM3.5 model was specifically developed for the simulation of the climate of the stratosphere. The model and the specifics of the 20 year integration were also described in Part I (MB94). Note that climatological sea surface temperatures were used. This is know to reduce the variability in the tropical atmosphere. However, the focus of the present work was on middle-high latitude low frequency variability, that is known to be captured also in simulations without varying sea surface temperatures (Lau and Nath, 1987, Bengtsson et al., 1994). In addition, prior to using a general circulation model in any sensitivity study, it is important to evaluate the variability associated with internal dynamical and physical processes.

The March-May zonal mean temperature and zonal wind are found to be reasonably well captured by the ECHAM3.5 model. In particular, the Northern hemisphere strato-

sphere is characterized by very weak westerly winds and high interannual variability in good agreement with the NMC-CAC global analyzed observations. This result is consistent with the successful simulation during February (MB94) and suggest that the Northern hemisphere polar vortex breakdown occurs in a realistic way in the model. Preliminary results of the daily evolution of meteorological fields during February and March from the ECHAM3.5 simulation (to be presented in a following report) indicate that the late winter simulated variability is associated with sudden warmings of the high-latitude middle stratosphere, thus supporting the above conclusions.

In the Southern hemisphere, the simulation of the polar cooling during March-May proceeds realistically at middle latitudes. However, in May the simulated zonal mean temperature is too low southward of 70°S, suggesting that a cold polar bias has already developed by late autumn. Also in the Northern hemisphere the simulated polar lower stratosphere is already too cold in autumn. Nevertheless, the quasi-stationary planetary wave pattern typical of the Northern hemisphere winter develops in a realist way in the model.

Given the tendency of general circulation models to produce extremely cold temperatures and strong westerly winds during the Antarctic polar night, the JJA winter season is usually difficult to simulate (Deque at al., 1994; Hamilton et al. 1995). A cold bias at the South Pole in the stratosphere occurs in the ECHAM3.5 simulation also, although of relatively moderate amplitude (about 10-20°K) and vertical extension. The time average of the JJA mean zonal wind is also relatively good, with deviations from the observed climatology of at most 20 ms^{-1}. The westerly wind bias during JJA is strongly influenced by the August climatology, when in the simulation the westerly jet does not close off in the upper stratosphere as indicated by the NMC-CAC analyzed observations.

The relative success of the current simulation of the climatological zonal mean circulation during the JJA winter is caused by the downward influence of the upper layer Rayleigh friction applied in the mesosphere in the ECHAM3.5 model. Short trial simulations with a substantially reduced damping coefficient of the upper layer Rayleigh friction were indeed characterized by colder temperatures and stronger westerly winds in the Southern hemisphere stratosphere. Although the mesospheric Rayleigh friction may be too crude to take into account the detailed effects of gravity wave breaking, the model response in the stratosphere is in agreement with the interpretation that small scale wave activity in the mesosphere plays a dominant role in regulating the strength of the general circulation also in the stratosphere (Haynes et al. 1991; McIntyre, 1992; Garcia and Boville, 1994).

In comparison with the DJF winter variability, the JJA winter variability is substantially smaller, especially at high latitudes and in the lower stratosphere. Although, the simulated JJA variability underestimates that observed, the poleward shift of the subtropical

variability maximum in zonal mean zonal wind is captured by the model. The NMC-CAC data indicates that from June to August in the upper stratosphere the zonal mean zonal winds are decreasing while the westerly jet core moves poleward and downward. Moderately high interannual variability is associated with this movement of the stratospheric jet, usually a rapid change occurring any time during JJA winter. In the model, the climatological westerly jet is instead centered at about 55°S throughout all the JJA season and the variability appears to be associated only with changes in the wind strength on the equatorward side of the polar night vortex.

The arising of some significant discrepancies between the model results and the NMC-CAC analyzed observations during the SON spring indicates that in the Southern hemisphere the simulation does not reproduce the basic characteristic of the final vortex breakdown. In the upper stratosphere, for instance, during the SON spring the simulated climatological zonal mean winds are about twice that observed and the westerly jet does not close in the model. The model fails to reproduce the poleward and downward motion of the westerly jet characteristic of the Southern hemisphere vortex breakdown in the NMC-CAC data. Among other causes, the reason for this discrepancy may be related to the role played by quasi-stationary planetary waves during the austral autumn. In their observational study about the stratospheric final warming in the Southern hemisphere, Mechoso et al. (1988) found indeed that during October the polar vortex breakdown was usually associated with the formation of a strong anticyclone located somewhere between 90°E and 180°E. This feature emerges as a well defined quasi-stationary planetary wave in the October NMC-CAC climatology of the lower stratosphere (with some interannual variability associated with it), while it is virtually absent in the model. Consequently, also the simulated variability during SON is strongly distorted. Presumably, the lack of quasi-stationary planetary waves in the model is associated with the low horizontal resolution (T21) used in the present simulation and therefore a misrepresentation of the large scale orographic forcing associated with the Antarctic continent. Further experimentation and analyses of the tropospheric and stratospheric circulations in the Southern hemisphere at different horizontal resolutions are therefore needed.

In MB94 it was suggested that an alleviation of the cold polar bias in the Northern hemisphere winter may be achieved by including a subgrid scale parametrization of the orographic gravity wave drag (see for instance Boville, 1991). However, an improvement of the simulation during the JJA winter and SON spring might involve the use of a more sophisticated gravity wave drag parametrization, including a spectrum of gravity waves (arising from a variety of sources) as in the parametrizations proposed by Hines (1991) and Fritts and Lu (1993). In addition, the current ECHAM3.5 model would have to be extended to at least the mesopause, in order to properly include the effects of such a generalized gravity wave drag parametrization. Development and experimentation addressing the gravity wave drag issue with a vertically extended version of the current ECHAM3.5 model are in progress.

Acknowledgements

The authors would like to thank William J. Randel for providing his compilation of the NMC-CAC global analyses. The technical assistance of colleagues at DKRZ and MPI is gratefully acknowledged.

References

Andrews, D. G., J. D. Mahlman, and R. W. Sinclair, 1983: Eliassen-Palm diagnostics of wave-mean flow interaction in the GFDL SKYHI general circulation model. *J. Atmos. Sci.*, **40**, 2768-2784.

Barnett, J. J., and M. Corney, 1985: Middle atmosphere reference model derived from satellite data. *MAP Handbook,* **16**, 47-85.

Bengtsson, L., K. Arpe, E. Roeckner, U. Schulzweida, 1994: Climate predictability experiments with a general circulation model. *MPI Report*, **145**, 45 pp

Boville B. A., 1991: Sensitivity of simulated climate to model resolution. *J. Climate,* **4**, 469-485.

Deque, M., C. Dreveton, A. Braun and D. Cariolle, 1994: The ARPEGE/IFS atmospheric model: A contribution to the French community climate modelling. *Climate Dynamics*, **10**, 249-266.

Farman, J. C., B. G. Gardiner and J. D. Shanklin, 1985: Large losses of total ozone in Antarctica reveal seasonal ClO_x/NOl_x interaction. *Nature,* **315,** 207-210.

Fels, S. B., J. D. Mahlman, M. D. Schwarzkopf, and R. W. Sinclair, 1980: Stratospheric sensitivity to perturbations in ozone and carbon dioxide: radiative and dynamical response. *J. Atmos. Sci.*, **37**, 2265-2297.

Finger, F. G., M. E. Gelman, J. D. Wild, M. L. Chanin, A. Hauchecorne and A. J. Miller, 1993: Evaluation of NMC upper-stratospheric temperature analyses using rocketsonde and lidar data. *Bull. Am. Met. Soc.,* **74**, 789-798.

Fritts, D.C., and W. Lu, 1993: Spectral estimates of gravity wave energy and momentum fluxes. Part II: Parametrization of wave forcing and variability. *J. Atmos. Sci.*, **50**, 3695-3713.

Garcia, R. R., and B. A. Boville, 1994: "Downward Control" of the mean meridional circulation and temperature distribution of the polar winter stratosphere, *J. Atmos. Sci.*, **51**, 2238-2245.

Hamilton, K., 1995: Interannual variability in the Northern Hemisphere winter middle atmosphere in control and perturbed experiments with the GFDL SKY general circulation model. *J. Atmos. Sci.*, **52**, 44-66.

Hamilton, K., R. J. Wilson, J. D. Mahlman and L. J. Umscheid, 1995: Climatology of the SKYHI troposphere-stratosphere-mesosphere general circulation model. *J. Atmos. Sci.*, **52**, 5-43.

Haynes, P. H., C. J. Marks, M. E. McIntyre, T. G. Shephered, and K. P. Shine, 1991: On the "Downward Control" of extratropical diabatic circulations by eddy-induced mean zonal forces. *J. Atmos. Sci.*, **48**, 651-678..

Hines, C. O., 1991: The saturation of gravity waves in the middle atmosphere. Part II: Development of Doppler-spread theory. *J. Atmos. Sci.*, **48**, 1360-1379.

Hirota, I., 1980: Observational evidence of the semiannual oscillation in the tropical middle atmosphere. *Pure Appl. Geophys.*, **118**, 217-238.

James, I.N., 1988: On the forcing of planetary-scale Rossby waves by Antarctica. *Quart. J. Roy. Meteor. Soc.*, **114**, 619-637.

Lau, N-C. and M. J. Nath, 1987: Frequency dependence of the structure and temporal development of wintertime tropospheric fluctuation. Comparison of a GCM simulation with observations. *Mon. Wea. Rev.*, **115**, 251-271.

Manzini, E., 1994: Modelling of the stratosphere with the ECHAM general circulation model. *Proc. ECMWF/WCRP workshop: Stratosphere and numerical weather prediction*, 171-191.

Manzini, E. and L. Bengtsson, 1994: Stratospheric climate and variability from a general circulation model and observations. Part I: Results for the December-February season. *MPI Report*, **148**, 38 pp

McIntyre, M. E., 1992: Atmospheric dynamics: Some fundamentals, with observational implications. *Proc. Int. School Phys. "Enrico Fermi" CXV Course: The use of EOS for studies of atmospheric physics.* (Ed.s J. C. Gille and G. Visconti) North-Holland, 313-386.

Mechoso, C. R., D. L. Hartmann and J. D. Farrara, 1985: Climatology and interannual

variability of wave, mean-flow interaction in the southern hemisphere. *J. Atmos. Sci*, **42**, 2189-2206.

Mechoso, C. R., A. O'Neill, V. D. Pope and J. D. Farrara, 1988: A study of the stratospheric final warming of 1982 in the southern hemisphere. *Quart. J. Roy. Meteor. Soc.*, **114**, 1365-1384.

Morcrette, J. J., 1991: Radiation and cloud radiative properties in the European Centre for Medium Range Weather Forecasts forecasting system. *J. Geophys. Res.*, **96**, 9121-9132.

Randel, W. J., 1988: The seasonal evolution of planetary waves in the southern hemisphere and troposphere. *Quart. J. Roy. Meteor. Soc.*, **114**, 1385-1409.

Randel, W. J., 1992: Global atmospheric circulation statistics, 1000-1 mb. *NCAR Technical Note TN-366+STR*, 256 pp.

Rasch, P. J., and D. L. Williamson, 1990: Computational aspect of moisture transport in global models of the atmosphere. *Quart. J. Roy. Meteor. Soc.*, **116**, 1017-1090.

Reed, R.J., 1966: Zonal wind behavior in the equatorial stratosphere and lower mesosphere. *J. Geophys. Res.*, **71**, 4223-4233.

Rind, D., R. Suozzo, N. K. Balachandran, 1988a: The GISS global climate middle atmosphere model. Part II: Model Variability due to interactions between planetary waves, the mean circulations, and gravity wave drag. *J. Atmos. Sci.*, **45**, 371-386.

Rind, D., R. Suozzo, N. K. Balachandran, A. Lacis and G. R. Russel, 1988b: The GISS global climate middle atmosphere model. Part I: Model structure and climatology. *J. Atmos. Sci.*, **45**, 329-370.

Roeckner, E., K. Arpe, L. Bengtsson, S. Brinkop, L. Dümenil, M. Esch, E. Kirk, F. Lunkeit, M. Ponater, B. Rockel, R. Sausen, U. Schlese, S. Schubert, W. Windelband, 1992: Simulation of the present-day climate with the ECHAM model: Impact of model physics and resolution. *MPI Report*, **93**, 172 pp.